

1     **Improved energy conversion performance of a novel design of concentrated photovoltaic**  
2             **system combined with thermoelectric generator with advance cooling system**

3     Abdelhak Lekbir<sup>a\*</sup>, Samir Hassani<sup>b</sup>, Mohd Ruddin Ab Ghani<sup>a</sup>, Chin Kim Gan<sup>a</sup>, Saad Mekhilef<sup>c</sup>,  
4     R. Saidur<sup>b,d</sup>

5  
6     <sup>a)</sup> Faculty of Electrical Engineering, Universiti Teknikal Malaysia Melaka, Hang Tuah  
7     Jaya, 76100 Durian Tunggal, Melaka, Malaysia.

8     <sup>b)</sup> Research Centre for Nano-Materials and Energy Technology (RCNMET), School of Science  
9     and Technology, Sunway University, No. 5, Jalan Universiti, Bandar Sunway, Petaling Jaya,  
10    47500 Selangor Darul Ehsan, Malaysia

11    <sup>c)</sup> Power Electronics and Renewable Energy Research Laboratory (PEARL), Department of  
12    Electrical Engineering, University of Malaya, 50603 Kuala Lumpur, Malaysia

13    <sup>d)</sup> Department of Engineering, Lancaster University, Lancaster, LA1 4YW, UK

14  
15    \*Corresponding author  
16    (lekbirabdelhak@gmail.com)

17  
18    **Abstract:**

19    Most of the incident solar energy on a PV panel is converted into waste heat. This consequently  
20    reduces the efficiency of PV system. Therefore, if certain portion of this waste heat can be  
21    utilized adding a thermoelectric generator (TEG) in the PV panel endowed by an efficient  
22    cooling system, the output performance of the system can be improved significantly. In this  
23    study, a new configuration of nanofluid-based PV/T-TEG hybrid system with cooling channel is  
24    proposed to convert certain portion of waste heat to electrical energy in order to improve the  
25    overall efficiency of hybrid system. Thus, the nanofluid acts as a coolant and absorbs the heat  
26    from the back side of TEG module raising its gradient of temperature, as well as the overall  
27    performance of the system. Through a numerical modelling approach, performance of the  
28    proposed innovative design has been investigated and compared with the conventional solar-  
29    harvesting technology systems. At the optimum value of solar concentration  $C$ , and maximum  
30    operating temperature of  $35^{\circ}\text{C}$ , the obtained results reveal that the electrical energy in NCPV/T-

1 TEG configuration has been found higher by ~10 %, ~47.7 % and ~49.5 % against NCPV/T,  
 2 CPV and CPV/TEG-HS systems, respectively. Overall, the proposed design of NCPV/T-TEG  
 3 hybrid system has potential for further development in high-concentration solar systems.

4 **Keywords:** PV/T; Thermoelectric Conversion; Nanofluid; Energy Conversion; Exergy.

---

### Nomenclature

$A$	<i>area, m<sup>2</sup></i>	<b>Greek symbols</b>
$a_{teg}$	<i>cross-sectional area of a P or N leg, m<sup>2</sup></i>	$\alpha$ <i>absorption coefficient</i>
$C$	<i>solar concentration</i>	$\alpha_{teg}$ <i>Seebeck coefficient, V/K</i>
$D_h$	<i>hydraulic diameter, m</i>	$\beta'$ <i>temperature coefficient, K<sup>-1</sup></i>
$e$	<i>electron charge, <math>1.6021 \times 10^{-19}</math> °C</i>	$\Delta T$ <i>temperature gradient, K</i>
$e_n$	<i>nanofluid thickness, m</i>	$\Delta_x$ <i>spatial step, m</i>
$G$	<i>solar radiation Wm<sup>-2</sup></i>	$\varepsilon$ <i>emissivity</i>
$h$	<i>heat transfer coefficient, Wm<sup>-2</sup> K<sup>-1</sup></i>	$\eta$ <i>efficiency</i>
$hr$	<i>radiation transfer coefficient, Wm<sup>-2</sup> K<sup>-1</sup></i>	$\tau$ <i>transmittance</i>
$L_c$	<i>characteristic length, m</i>	$\lambda$ <i>wavelength, <math>\mu\text{m}</math></i>
$l_{teg}$	<i>height of TEG, m</i>	$\phi$ <i>volume fraction</i>
$l$	<i>collector length, m</i>	<b>Subscripts</b>
$\dot{m}$	<i>mass flow rate, kg s<sup>-1</sup></i>	$a$ <i>air gap</i>
$n_{teg}$	<i>numbers of PN junction</i>	$c$ <i>cover glass</i>
$Q_{TEG,h}$	<i>energy that passed in hot side of the TEG, W</i>	$n$ <i>nanofluid</i>
$Q_{TEG,c}$	<i>energy that passed in cold side of the TEG, W</i>	$am$ <i>ambient</i>
$R$	<i>thermal resistance kW<sup>-1</sup></i>	$p$ <i>plate</i>
$r_{teg}$	<i>electrical resistivity of P or N junction, <math>\Omega\text{m}</math></i>	$bc$ <i>back cover</i>
$T_{am}$	<i>ambient temperature K</i>	$eq$ <i>equivalent</i>
$T_{teg,h}$	<i>hot side temperature K</i>	
$T_{teg,c}$	<i>cold side temperature K</i>	
$V$	<i>velocity, m s<sup>-1</sup></i>	
$ws$	<i>wind speed</i>	

## Abbreviations

<i>PV</i>	<i>Photovoltaic</i>
<i>TEG</i>	<i>Thermoelectric Generator</i>
<i>PV/T</i>	<i>Photovoltaic/Thermal</i>
<i>PV/T-TEG</i>	<i>Photovoltaic/Thermal-Thermoelectric Generator</i>
<i>NCPV/T</i>	<i>Nanofluid-based Concentrated Photovoltaic/Thermal</i>
<i>NCPV/T-TEG</i>	<i>Nanofluid-based Concentrated Photovoltaic/ Thermal-Thermoelectric Generator</i>
<i>HS</i>	<i>Heat Sink</i>

---

1

## 2 **Introduction:**

3 Renewable energy is a promising source of energy as it is clean and environmental friendly  
4 compared to fossil fuel-based resources. According to Global Trends in Renewable Energy  
5 Investment report, by the year 2017, approximately 55% investment in energy installation was  
6 based on renewables energy resources which is roughly more than double invested in fossil fuel  
7 based power generation [1]. Several renewable resources are available on earth, and sun is the  
8 most promising renewable energy resources to meet the future world energy demand. Energy  
9 converter devices that use solar energy as primary resources could be the most effective solution  
10 to avoid pollution and reduce the greenhouse effect.

11 According to the Renewables 2017 Global Status Report[2], about 307.8 GW represent the total  
12 electric power capacity generated from the solar energy in 2016. Nearly 98% of this generated  
13 power was from PV systems. This is because the annual market of the solar panel witnessed a  
14 significant increase nearly to 50%, which rises the global total PV electrical energy to achieve  
15 303 GW.

16 However, PV cells technology faces several technical challenges such as its low performance  
17 under extreme weather conditions [3]. Using a solar concentrator technology, the PV cells output  
18 enhances, which might reduce the manufacturing [4] and electricity cost [5] of the PV  
19 technology. However, under high irradiation, the PV module temperature rises rapidly due to the  
20 excess heat, consequently their efficiency drops drastically at elevated temperature. Therefore,

1 removing heat by cooling the PV cells and utilizing certain portion using TEG attached to the PV  
2 panels is a crucial approach to boost the energy production in a PV power plant. Several methods  
3 and approaches were proposed by researchers to enhance PV cells performance. A summary of  
4 these works is available in the review paper published by Makki et al. [6].

5 The thermoelectric conversion system is another alternative mechanism to generate electricity  
6 using low grade heat. It allows the generation of a clean electricity from a source of heat through  
7 a thermoelectric generator device under Seebeck effect, i.e. presence of gradient of temperature  
8 is required. Serval researchers' published works recommended hybrid PV modules and TEG in  
9 one system device. Thus, the TEG is placed in the back of the PV cells to absorb and convert the  
10 excess heat to electricity. This modus operandi is a unique approach to maximize the overall  
11 conversion efficiency of PV system.

12 Sark et al.[7] conducted a study on PV module under high irradiance condition. The PV cells  
13 temperature reached  $60 - 80^{\circ}\text{C}$  in their study. By integrating a TEG module in the backside of  
14 the PV module, authors noticed an improvement of 8 to 23% on the efficiency of the PV system,  
15 depending on the proprieties of TEG materials used.

16 Lin et al [8] analyzed the effect of solar irradiance, load resistances and the TEG parameter on  
17 the performance of a PV/TEG hybrid system. The TEG module was used to improve the  
18 conversion efficiency of solar energy as well as to increase the electrical power output.  
19 Kossyvakis et al [9] examined theoretically and experimentally the electrical output of a  
20 PV/TEG hybrid system. By using a TEG device with a thermoelement geometry, the overall  
21 performance improvement was achieved 22.5% and 30.2% for poly-Si and dye-sensitized solar  
22 cells, respectively. Zhu et al [10] combined PV/TEG modules to reduce the energy losses in the  
23 PV system. Authors found that the overall efficiency of the hybrid system achieved 25% , while  
24 the electrical efficiency of the PV module alone, i.e. without TEG module reached 19 % only.

25 Li et al [11][12] investigated theoretically and experimentally a PV/TEG hybrid system. The PV  
26 module and the TEG generator were connected by using a micro-channel heat pipe for heat  
27 removal purpose. To increase the gradient of temperature between TEG's both sides, a heat sink  
28 was placed in the TEG's cold side. A comparison in terms of electrical performance between the  
29 proposed PV/TEG and a conventional PV module under deferent ambient conditions was  
30 reported as well. Under the concentration ratio of 8x, and wind speed of  $8\text{ m/s}$ , the electrical

1 efficiency of the TEG device improved by 0.82% based on  $\Delta T = 59.6 \text{ }^\circ\text{C}$ . This resulted in a  
2 significant increase in overall electrical output of the hybrid system compared to the  
3 conventional PV system.

4 Mohsenzadeh et al. [13] designed a novel hybrid PV/T system combined with a TEG generator  
5 to increase the overall system efficiency. In addition, a parabolic concentrator was used to  
6 intensify the solar radiation. The overall efficiency of the CPV/T-TEG system found to be  
7 ~60% and 47.30% with and without the glass cover, respectively. Thermal energy represented  
8 90.53 % of the total generated power, while electrical energy represented 9.47% only. The TEG  
9 generator provided 3.3% from the total generated electrical energy. Soltani et al.[14] proposed a  
10 new cylindrical PV/TEG system operated under parabolic through collector. Water was used for  
11 cooling with the mass flow rate  $0.03 \text{ kg/s}$ . Authors found that the TEG generator provided only  
12  $2.3 \text{ W}$  from the total  $22.714 \text{ W}$  electrical power delivered by the whole system.

13 Previous studies have proved the feasibility of combining PV with TEG technology as a hybrid  
14 system, however, several literature works highlighted that the combining PV with TEG generator  
15 is economically ineffective approach compared to conventional PV generator systems [11][15]  
16 due to; low energy conversion efficiency of TEG technology ( $\sim 6\text{--}8\%$ ), limitation of the  
17 amount of generated power at low gradient of temperature [16], higher cost of the high end TEG  
18 module and the large cooling equipment cost. In addition, most of PV/TEG hybrid system using  
19 heat sink as cooling system are non-uniform in the cooling process due to the fact that heat sink  
20 relies on the ambient conditions i.e. it achieves higher performance only during windy days.  
21 Furthermore, some of the PV/TEG systems use water as a coolant, however water as well has  
22 some limitations in its thermophysical properties particularly under high working temperature.  
23 This is to conclude that PV/TEG performance is highly depending on the quality of cooling  
24 process.

25 Ideally, TE material should have a large seebeck coefficient, high electrical conductivity and a  
26 low thermal conductivity. In the real-world application of PV/TEG hybrid system, with low  
27 cooling performance, the TEG increases the temperature of the PV module due the low thermal  
28 conductivity of the TE material i.e. poor heat transfer coefficient. Consequently, the degradation  
29 of PV performance will persist and the gain in energy produced by the TEG will be insignificant.

1 Therefore, it is obvious that using an effective cooling system to cool down the TEG and PV  
2 cells is highly recommended.

3 Researchers previously used cooling system to keep PV cells temperature as low as possible in  
4 order to maintain higher efficiency. Generally, water and air are used as coolants in this case.  
5 However, due to their poor thermal properties and with the recent development in nanomaterial  
6 science, researchers proposed the use of nanofluids as effective heat transfer fluids due to their  
7 superior thermal properties. Thus, several research works in nanofluids field proved that  
8 nanofluid is an excellent heat carrier in several heat transfer applications either for cooling or  
9 heating.

10 Al-Shamani et al. [17] designed, fabricated and tested a PV/T collector that consists of specially  
11 designed rectangular tube absorber attached under the photovoltaic module. The PVT collector  
12 was experimentally tested under outdoor Malaysian tropical climate conditions with different  
13 types of nanofluids. They reported that under  $1000 \text{ W/m}^2$ , the temperature of the PV cells was  
14  $50^\circ\text{C}$  when water is used as a coolant. However, by using SiC nanofluid as a coolant, the  
15 temperature was dropped to  $42.6^\circ\text{C}$  and the efficiency found to be improved up to 13.5%.

16 Rejeb et al. [18] performed an experimental and numerical study to evaluate the performance of  
17 a photovoltaic thermal (PV/T) nanofluid based collector. The results indicated that using  
18 Cu/water nanofluids gives the best thermal and electrical efficiency compared to water. Authors  
19 found that using Cu/H<sub>2</sub>O as a coolant in PV/T could generate an annual thermal and electrical  
20 energy of 791 and 285  $\text{kWh/m}^2$  respectively. However, 488 and 278  $\text{kWh/m}^2$ , respectively,  
21 can be produced using water as a coolant.

22 Hassani et al. [19] proposed a new cascading nanofluid-based PV/T configuration with two  
23 separate channels, where one channel controls the optical properties and the other enhances heat  
24 removal from the PV cells. In the first channel, optical nanofluid acts as a liquid optical band-  
25 pass filter above the PV cells while in the second channel, thermal nanofluid, removes heat from  
26 the back of the PV cells. The proposed system has been simulated for both GaAs- and Si-based  
27 PV cells at various concentration ratios. According the obtained results, the overall system  
28 efficiency with GaAs (at  $C = 160$ ) and Si (at  $C = 100$ ) has found to be improved by ~

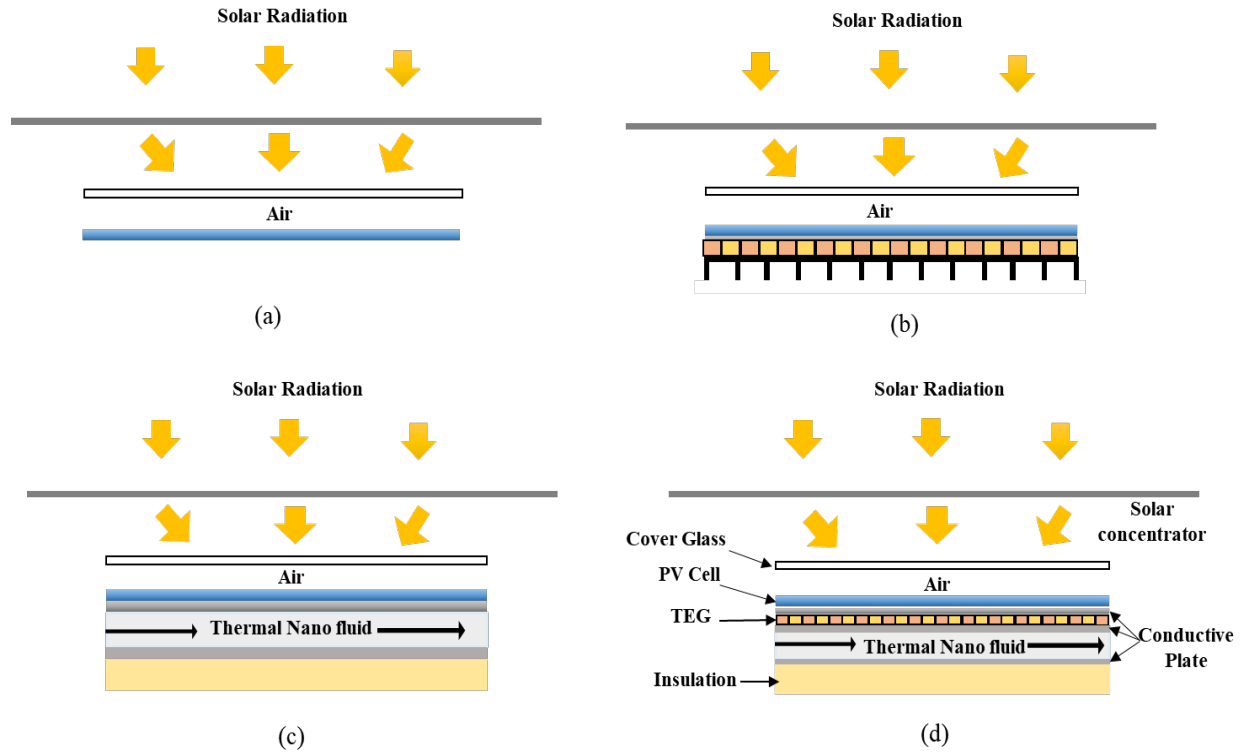
1 5.8% and  $\sim 4.6\%$ , respectively, by increasing the volume fraction of the thermal nanofluid from  
2 0.001 to 1.5%. It has to be noted that TEG was not used in this configuration.

3 Based on the literatures study, the hybrid PV/TEG system was reported in several works. Most  
4 of these studies used heat sink in the TEG's cold side to create a large gradient of temperature  
5 and intensify the heat transfer between the PV cells and the TEG module. In other words, the  
6 heat sink improves PV cells cooling and TEG performance. However, the removed heat in this  
7 case is released to the environment. In energy conversion point of view, this energy is lost which  
8 reduces the overall efficiency of the system. Moreover, in heat transfer point of view, heat sink  
9 has lower cooling potential than liquids. Therefore, in the present paper a novel design of  
10 nanofluid based PV/T-TEG hybrid system is proposed to utilize the waste heat. Thus, a nanofluid  
11 based coolant has been used instead of a heat sink. Aim of this approach is to boost both PV and  
12 TEG performance, and at the same time utilizing waste heat in the form of useful energy.  
13 Overall, this paper presents a rigorous study of an improved PV/T-TEG design, which opens up  
14 a new approach for hybrid solar collectors.

## 15 **2. Methods:**

16 The description of the physical NCPV/T-TEG system proposed in this study is presented in  
17 Fig.1(d). The other three configurations are presented in Fig. 1 (a)-(c) to compare the  
18 performance of proposed new design (Fig. 1(d)) which is the focused of the present study.

19 The components and specifications of the four configurations are presented in Table 1.



1

2 **Figure 1:** Physical description; (a) conventional CPV; (b) CPV/TEG-HS hybrid system; (c)  
 3 NCPV/T hybrid system; (d) proposed NCPV/T-TEG hybrid system.

4 **Table 1:**

5 Characteristics of all four configurations

	CPV	CPV/TEG-HS	NCPV/T	NCPV/T-TEG
Concentrator	✓	✓	✓	✓
Cover glass	✓	✓	✓	✓
PV module	✓	✓	✓	✓
Conductive plate 1		✓	✓	✓
TEG generator		✓		✓
Heat sink		✓		
Conductive plate 2			✓	✓
Nanofluid based coolant			✓	✓
Conductive plate 3				✓
Insolation			✓	✓

6

7 The necessary input parameters involved in this study has been presented in Table 2.



1 **Table 2**

2 Input parameters for the PV/T-TEG

Parameter	Value
$A$	$1 \text{ m}^2$
$L$	$1 \text{ m}$
$L_c$	$0.25 \text{ m}$
$D_h$	$0.0392 \text{ m}$
$e_n$	$0.2 \text{ m}$
$\Delta_x$	$0.25 \text{ m}$
$\alpha_c$	$0.05$
$\alpha_{pv}$	$0.945$
$\varepsilon_c$	$0.9$
$\varepsilon_{pv}$	$0.9$
$R_p$	$5.71 \times 10^{-6} \text{ K/W}$
$T_{am}$	$298 \text{ K}$
$ws$	$1 \text{ m/s}$
$\dot{m}$	$0.0104 \text{ kg/s}$
$\phi_n$	$0.1\%$ , (0.21wt %)
$\alpha_{teg}$	$187 \times 10^{-6} \text{ V/K}$
$a_{teg}$	$1 \times 10^{-8} \text{ m}^2$
$n_{teg}$	$2 \times 241$
$r_{teg}$	$1.64 \times 10^{-5} \Omega\text{m}$
$l_{teg}$	$3.4 \times 10^{-3} \text{ m}$
$K_{teg}$	$1.46 \text{ W/mK}$

3

4 **2.1 Mathematical models**

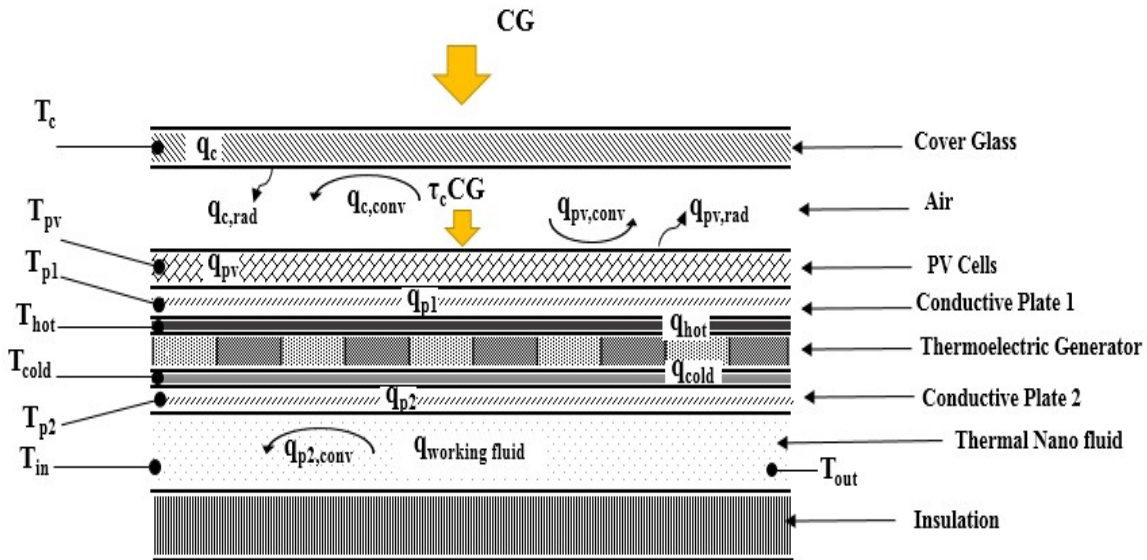
5 A detailed numerical model of the proposed nanofluid based PV/T-TEG was developed to  
6 investigate its performance. Thus, equations related to thermal unit (i.e. nanofluid channel), PV  
7 cells, and TEG modules are coupled and solved simultaneously. A systematic study of the

1 salient operation parameters and the physical geometry were studied to examine the performance  
 2 of the NCPV/T-TEG system.

### 3 2.1.1 Thermal model

4 The thermal boundary conditions for each element of the proposed system are presented in Fig.  
 5 2. The solar radiation reaches the PV panel after crossing the Cover Glass (CG). A conductive  
 6 plate transfers the heat from the PV panel to the hot side of the TEG. To enhance the TEG  
 7 efficiency, an increase on the gradient of temperature between TEG hot and cold side is required.  
 8 Therefore, a thermal nanofluid with high cooling performance is placed in a channel under the  
 9 TEG module.

10



11

12 **Figure 2:** Configuration of the physical NCPV/T-TEG system

13 The thermal model used in this study was derived by applying the first law of thermodynamics  
 14 (i.e. the energy balance equation) for each element of the proposed NCPV/T-TEG hybrid system.  
 15 The present model is based on the previous work of Hassani et al. [19], [20]. It has to be noted  
 16 that in Hassani et al.'s models, TEG was not included. Therefore, this is the novelty of the  
 17 proposed model to utilize some of the waste heat to improve the overall efficiencies of the  
 18 proposed design. The energy balance equation is expressed by Eq. (1).

$$\frac{\partial U}{\partial t} = \dot{Q}_{in} - \dot{Q}_{out} + \dot{Q}_g \quad (1)$$

1

2 Where:  $\partial U/\partial t$  the change in the internal energy.  $\dot{Q}_{in}$  and  $\dot{Q}_{out}$  are the heat transfer rate into and  
 3 out of the system, respectively,  $\dot{Q}_g$  is the heat generation rate into the system.

4 To simplify the thermal model used in this study, Table 3 summarizes the assumptions  
 5 considered in this study.

6

7

8

9 **Table 3:**

10 Assumptions considered in this study. Taken from [20]

Assumptions
1 Steady state
2 Normal incident irradiation
3 Uses a thin, uniform temperature cover glass
4 Thermophysical properties of the fluids are temperature dependent.
5 All working fluids remains liquid during operation.
6 Thermal energy is only transferred in the flow direction.
7 Cover glass, plate, and air gaps are independent of temperature.
8 Electrical pumping power is considered negligible due to low mass flow rates.

11 The temperature variation along the flow direction is also considered. Therefore, a backward  
 12 scheme for the spatial coordinate (x) is adopted to discretize the derived thermal energy balance  
 13 equations for each element of the NCPV/T-TEG system. The resulting discretized equations are  
 14 summarized in Table 4.

15

16 **Table 4:**

17 Energy balance equations of the NCPV/T-TEG system presented in Fig 2.

$$h_{c-a}(T_{a,i} - T_{c,i}) + hr_{c-pv}(T_{pv,i} - T_{c,i}) + \alpha_c CG - h_{eq(c-am)}(T_{c,i} - T_{am}) = 0 \quad (2)$$

$$hr_{pv-a}(T_{pv,i} - T_{a,i}) - h_{c-a}(T_{a,i} - T_{c,i}) = 0 \quad (3)$$

$$\tau_c C \int_{0.28 \mu m}^{2.5 \mu m} G_\lambda (\alpha_{pv} - \eta_{el}(1 - \beta'(T_{pv} - 298))) d\lambda = \frac{T_{pv,i} - T_{p,i}}{R_p} + hr_{c-pv}(T_{pv,i} - T_{c,i}) \quad (4)$$

$$\frac{T_{pv,i} - T_{p,i}}{R_p} - \frac{T_{p,i} - T_{TEG,h}}{R_{TEG}} = 0 \quad (5)$$

$$\frac{T_{p,i} - T_{TEG,h}}{R_{TEG}} - \frac{T_{TEG,h} - T_{TEG,c}}{R_{TEG}} = 0 \quad (6)$$

$$\frac{T_{TEG,h} - T_{TEG,c}}{R_{TEG}} - \frac{T_{TEG,c} - T_{p,i}}{R_p} = 0 \quad (7)$$

$$\frac{T_{TEG,c} - T_{p,i}}{R_p} - h_{p-n}(T_{p,i} - T_{n,i}) = 0 \quad (8)$$

$$h_{p-n}(T_{p,i} - T_{n,i}) - \dot{m}_c c p_n \frac{T_{n,i} - T_{n,i-1}}{l \Delta x} - h_{p-n}(T_{n,i} - T_{p2,i}) = 0 \quad (9)$$

$$h_{p-n}(T_{n,i} - T_{p2,i}) - \frac{T_{p2,i} - T_{i,i}}{R_i} = 0 \quad (10)$$

$$\frac{T_{p2,i} - T_{i,i}}{R_i} - \frac{T_{i,i} - T_{bc,i}}{R_{bc}} = 0 \quad (11)$$

$$\frac{T_{i,i} - T_{bc,i}}{R_{bc}} - h_{eq(bc-am)}(T_{bc} - T_{am}) = 0 \quad (12)$$

1

## 2 2.1.2 Electrical and thermal efficiencies models

3 The output power of the PV module and the TEG generator,  $P_{PV}$  and  $P_{TEG}$  respectively, are  
4 directly related to the intensity of solar radiation and the cooling rate. The maximal electrical  
5 power generated by the hybrid system NCPV/T-TEG is expressed as below:

$$P_{HYB} = P_{PV} + P_{TEG} \quad (13)$$

6 where  $P_{PV}$  is the electrical energy generated by the PV module. It can be expressed as follow:

$$P_{pv} = \tau_c (1 - \beta'(T_{PV} - T_0)) \int_{0.28 \mu m}^{\lambda_g} \eta_{0,\lambda} G_\lambda d\lambda \quad (14)$$

7 where:  $\tau_c$  is the cover glass transmittance,  $T_0 = 298 K$  and the  $\beta'$  is the temperature coefficient,  
8  $\lambda_g$  is the maximum wavelength of the full solar spectrum up to  $2.5 \mu m$ ,  $\eta_{0,\lambda}$  is the spectral  
9 electrical efficiency of the Si PV cells at  $25^\circ C$ . , and taken from ref. [21]

10 Thus, the electrical efficiency of the PV cells for different configurations are calculated as  
11 follows based on [20]:

$$\eta_{PV} = \frac{\tau_c (1 - \beta'(T_{PV} - T_0)) \int_{0.28 \mu m}^{\lambda_g} \eta_{0,\lambda} G_\lambda d\lambda}{G} \quad (15)$$

1 The  $P_{TEG}$  is the electrical energy generated by the TEG module, and it is determined using Eq.  
 2 (16):

$$P_{TEG} = Q_{TEG,h} - Q_{TEG,c} \quad (16)$$

3 where  $Q_{TEG,h}$ ,  $Q_{TEG,c}$  are the thermal energy at hot and cold side of the TEG generator,  
 4 respectively.  $Q_{TEG,h}$  represents the heat received from the PV module. These are determined  
 5 using the following equations taken from reference [11]:

$$Q_{TEG,h} = 2n_{teg}\alpha_{teg}T_{teg,h} + 2n_{teg}\frac{a_{teg}k_{teg}}{l_{teg}}\Delta T - \frac{1}{2}I^2 2n_{teg}\frac{r_{teg}l_{teg}}{a_{teg}} \quad (17)$$

$$Q_{TEG,c} = 2n_{teg}\alpha_{teg}T_{teg,c} + 2n_{teg}\frac{a_{teg}k_{teg}}{l_{teg}}\Delta T + \frac{1}{2}I^2 2n_{teg}\frac{r_{teg}l_{teg}}{a_{teg}} \quad (18)$$

6 where, the  $\Delta T$  is the temperature gradient. The  $T_{teg,h}$  and  $T_{teg,c}$  is the hot and cold's side  
 7 temperature respectively,  $I$  is the current,  $n_{teg}$  is the numbers of PN junction,  $\alpha_{teg}$  is the  
 8 Seebeck coefficient,  $k_{teg}$  is the thermal conductivity of TEG,  $l_{teg}$  is the length of TEG,  $r_{teg}$  is the  
 9 electrical resistivity of P or N leg, and  $a_{teg}$  is the Cross-sectional area of P or N junction.

10 The electrical efficiency of TEG generator is given as below:

$$\eta_{TEG} = \frac{Q_{TEG,h} - Q_{TEG,c}}{Q_{TEG,h}} \quad (19)$$

11 After determining efficiency for PV and TEG module, the electrical efficiency of the hybrid  
 12 system proposed in this study can be calculated as follow:

$$\eta_{el} = \frac{P_{PV} + P_{TEG}}{C \times A \times G} \quad (20)$$

13 The thermal energy efficiency of the NCPV/T and NCPV/T-TEG system can be given as below:

$$\eta_{th} = \dot{m}_n \frac{cp_n(T_{n,out} - T_{n,in})}{C \times A \times G} \quad (21)$$

14 where the  $\dot{m}$  is the mass flow rate,  $cp$  is the specific heat of the nanofluid,  $C$  is the solar  
 15 concentration,  $A$  is the cross area and  $G$  is the solar irradiation.

### 16 2.1.3 Determination of the thermal conductivity of nanofluid:

17 In the present study, carbon nanotube (CNT) of diameter 15 nm suspended in water was chosen  
 18 to be used as a coolant in the cooling channel for the NCPV/T to cool down the PV cells, and in

1 NCPV/T-TEG configuration to improve the heat removal from the cold side of the TEG  
2 generator.

3 To optimize the nanofluid used as a coolant for both configurations NCPV/T and NCPV/T-TEG,  
4 a correlation developed by Hassani et al.[22] was used to optimize the thermal conductivity of  
5 the nanofluid. The remaining thermophysical properties of nanofluids were estimated using  
6 mathematical models reported in ref. [23].

#### 7 **2.1.4 Overall exergy analysis**

8 Electrical and thermal energy have different quality grades [20]. Electrical energy has a quality  
9 of exergy similar to its energy as electrical energy is a high-grade energy. However, the amount  
10 of thermal energy is lower than its exergy. The overall energy efficiency analysis is not effective  
11 compared to exergy efficiency analysis [24]. This is due to fact that, exergy efficiency analysis  
12 takes into consideration the concept of energy quality. Therefore, exergy analysis is considered  
13 in this study.

14 The exergy efficiency for each configuration can be given as follow:

$$\eta_{ex} = \eta_{el} \quad (22)$$

15 Eq. (22) is used for CPV and CPV/TEG-HS systems to calculate exergy efficiency.

$$\eta_{ex} = \eta_{el} + K\left(1 - \frac{T_0}{T_{n,out}}\right)\eta_{th} \quad (23)$$

16 Eq. (23) is used to calculate exergy efficiency for NCPV/T [20].

17

$$\eta_{ex} = \eta_{el} + K\left(1 - \frac{T_0}{T_{n,out}}\right)\eta_{th} \quad (24)$$

18 where:  $\eta_{el} = \frac{P_{PV} + P_{TEG}}{CAG}$  for CPV/TEG-HS and NCPV/T-TEG

19 Eq. (24) is used to calculate exergy efficiency for NCPV/T-TEG.

20

### 21 **3. Results and discussion:**

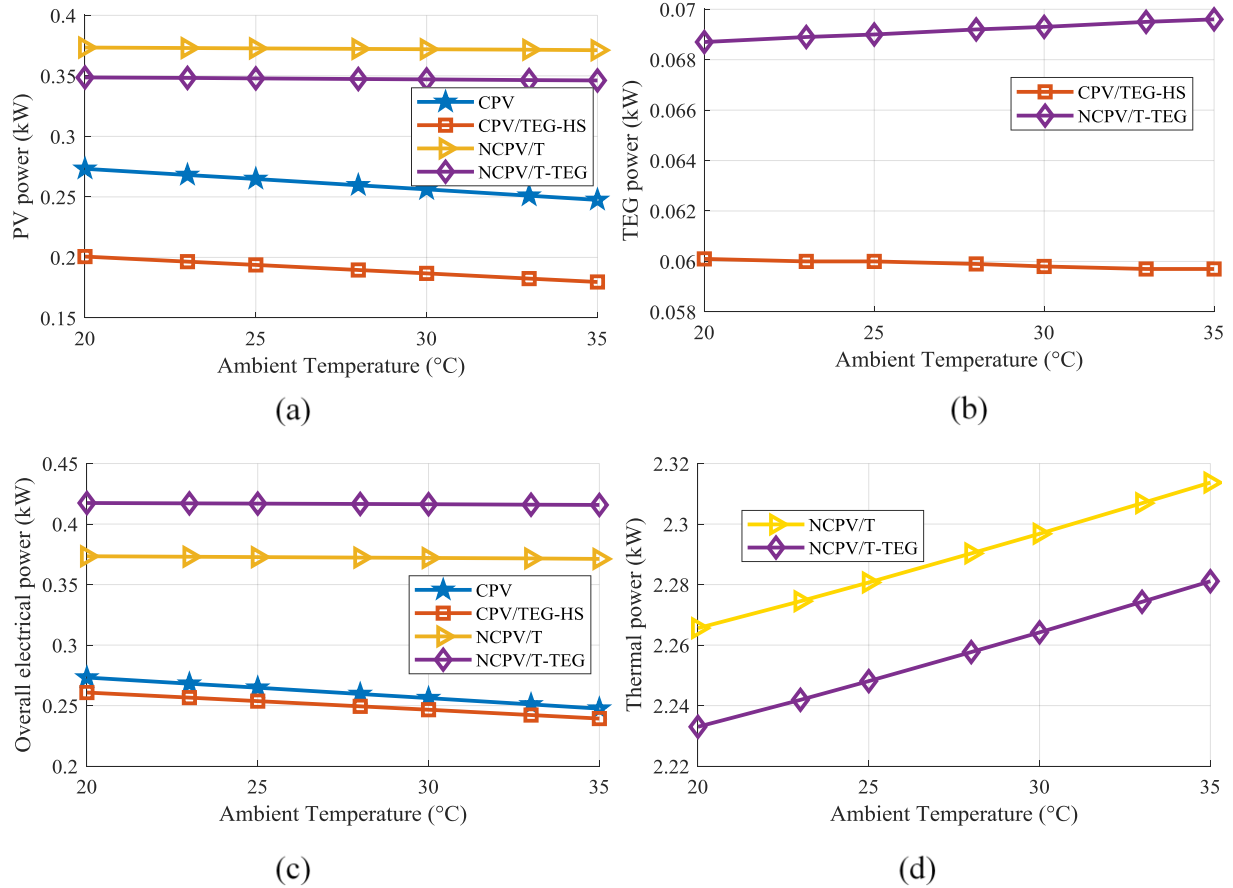
22 The proposed NCPV/T-TEG system in this study is an enhanced version of a nanofluid  
23 based coolant NCPV/T system reported in reference [20] by integrating a TEG module in the  
24 PV/T system which is the novel part of this work. To assess the thermal and electrical

1 performance of the proposed system, a comparative study was carried out with other 3  
 2 configurations presented in Fig. 1 (a)-(c). Thus, the proposed system has been numerically  
 3 investigated along with three other configurations namely; CPV stand alone, CPV/TEG-HS, and  
 4 NCPV/T hybrid system. The variation effect of solar concentration, wind speed, ambient  
 5 temperature, mass flow rate, and volume fraction of nanofluid on the thermal and electrical  
 6 performance was considered.

7

8 **3.1 The variation in ambient temperature:**

9 The variation of ambient temperatures could have a direct effect on the performance of the  
 10 all four configurations. Therefore, to analyze the output power of the four configurations, an  
 11 interval of ambient temperature from 20 °C to 35 °C was set as input in the computing algorithm.  
 12 The obtained output power of all four configuration with the variation of temperature was  
 13 presented in Fig.3.



14

1 **Figure 3:** Impact of ambient temperature variation on (a) PV electrical power output, (b) TEG  
2 electrical power output, (c) overall electrical power output and (d) thermal power output. The  
3 depicted data are calculated under the following conditions;  $w_s = 1.5 \text{ m/s}$ ,  $C = 4$ . In addition,  
4 for NCPV/T and NCPV/T-TEG the  $\dot{m}=0.0104\text{kg/s}$ ,  $\phi = 0.001$ .

5 From Fig. 3, it is obvious that the increase in ambient temperature has an inverse effect on the  
6 PV electrical performance for all of the studied configurations. This phenomenon is more  
7 pronounced in case of CPV and CPV/TEG-HS as shown in Fig.3(a) and (c), while the increase  
8 on ambient temperature has slightly a negligible effect in case of NCPV/T and NCPV/T-TEG.  
9 This is due to the fact that the cooling system in NCPV/T and NCPV/T-TEG performs better  
10 than CPV and CPV/TEG-HS. This better performance is also due the higher thermal  
11 conductivity of CNT based nanofluid used in NCPV/T and NCPV/T-TEG systems. Due to  
12 higher thermal conductivity, heat transfer or cooling capacity is better than other cooling system.  
13 For TEG module performance, the increase in ambient temperature has been found proportional  
14 to the electrical output of the TEG module in case of proposed NCPV/T-TEG system. This trend  
15 is found inversely proportional in case of CPV/TEG-HS as shown in Fig. 3(b). This is due to the  
16 increase in temperature in TEG's hot side and better cooling performance ensured by the  
17 nanofluid to keep the TEG's cold side temperature close to the ambient temperature leading to a  
18 positive increase on the TEG's gradient of temperature. This unique benefit is missing in case of  
19 CPV/TEG-HS due to the fact that the heat sink cannot bring the TEG's cold side lower than the  
20 ambient temperature because the latter is using wind and ambient temperature (i.e. heat  
21 convection) as a boundary condition.

22 Although the PV electrical output in NCPV/T system is higher than NCPV/T-TEG, the overall  
23 electrical performance in NCPV/T-TEG outperforms than all of the studied configurations as  
24 depicted in Fig. 3(c). It has to be noted that the TEG module in NCPV/T-TEG acts like a thermal  
25 barrier which slow down the cooling process leading to an increase in PV cells temperature,  
26 consequently to a decrease in their electrical efficiency.

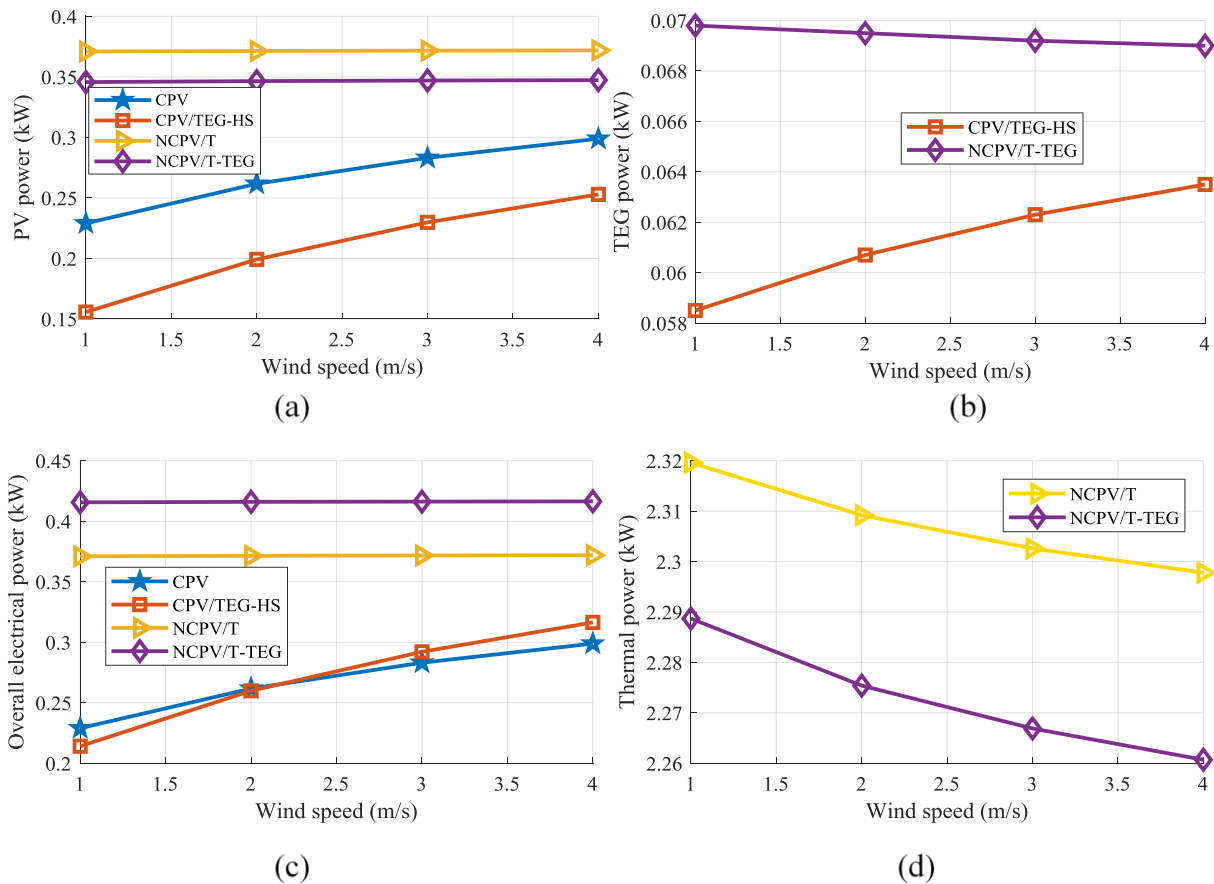
27 With regard to the thermal performance of the proposed system NCPV/T-TEG against  
28 NCPV/T, it can be seen form Fig 3(d) that more useful heat has been collected from NCPV/T  
29 than NCPV/T-TEG. This can be explained by the fact that a fraction of heat energy collected  
30 form PV cells in NCPV/T-TEG was turned into electrical energy via the TEG module and the



1 remaining portion has been carried out by the nanofluid, while the amount of heat generated by  
 2 the PV cells in NCPV/T has been fully collected by the nanofluid based coolant.

### 3 3.2 The variation in wind speed

4 Similar to ambient temperature, wind speed variation can affect the system performance either  
 5 negatively or positively. Therefore, the four configurations will be analyzed under an interval of  
 6 wind speed values from 1 to 4m/s. The obtained results are depicted in Fig.4.



7

8 **Figure 4:** Impact of wind speed variation on (a) PV electrical power output, (b) TEG electrical  
 9 power output, (c) overall electrical power output and (d) thermal power output. The depicted data  
 10 are calculated under the following conditions;  $T_{am} = 35^{\circ}C$ ,  $C = 4$ . In addition, for NCPV/T and  
 11 NCPV/T-TEG the  $\dot{m}=0.0104\text{kg/s}$ ,  $\phi = 0.001$ .

12 In contrast to the ambient temperature, wind speed has a positive effect on the electrical  
 13 performance of PV cells for all the studied configurations as shown in Fig. 4(a). The increase in

1 wind speed enhances the TEG electrical output for CPV/TEG-HS system as shown in Fig. 4(b)  
 2 because the wind speed in this case intensify the heat exchange in the heat sink which improves  
 3 its cooling process and lower TEG's cold side temperature ensuring a large gradient of  
 4 temperature. However, this is not the case for NCPV/T-TEG system where the increase in wind  
 5 speed turns down the TEG electrical efficiency. This is due to the fact that the wind speed  
 6 reduces the PV cells temperature in NCPV/T-TEG system which is the main source of heat for  
 7 the TEG's hot side.

8 The thermal performance in both configurations NCPV/T and NCPV/T-TEG has been negatively  
 9 affected by the increase in wind speed as shown in Fig. 4 (d). The convective heat transfer  
 10 between the system and the ambient has been intensified by increasing the wind speed leading to  
 11 a loss of considerable amount of useful heat to environment. This finding is in line with several  
 12 experimental works reported in the literature[25].

13 Although increasing wind speed has unwanted effect on the thermal performance of the proposed  
 14 system, the overall electrical output of NCPV/T-TEG offers the best performance compared to  
 15 other configurations as can be seen in Fig. 4(c).

### 16 3.3. Benefits of using solar concentrator system

17 This section is devoted in investigating the effect of solar concentration variation on PV cells'  
 18 temperature for the all case configurations, gradient of temperature for TEG module in  
 19 CPV/TEG-HS and NCPV/T-TEG systems, and nanofluid's temperature in NCPV/T and  
 20 NCPV/T-TEG. Thus, these different temperatures have been calculated solving equations  
 21 presented in Table 4 under the following operating conditions;  $T_{am} = 308 K$ ,  $ws = 1.5 m/s$ ,  
 22  $1 < C < 5$ ,  $\dot{m}=0.0104kg/s$  and  $\phi = 0.001$ . The obtained results are summarized in Table 5.

23 **Table 5:**

24 PV module and working fluid temperatures at various solar concentration ratio, C

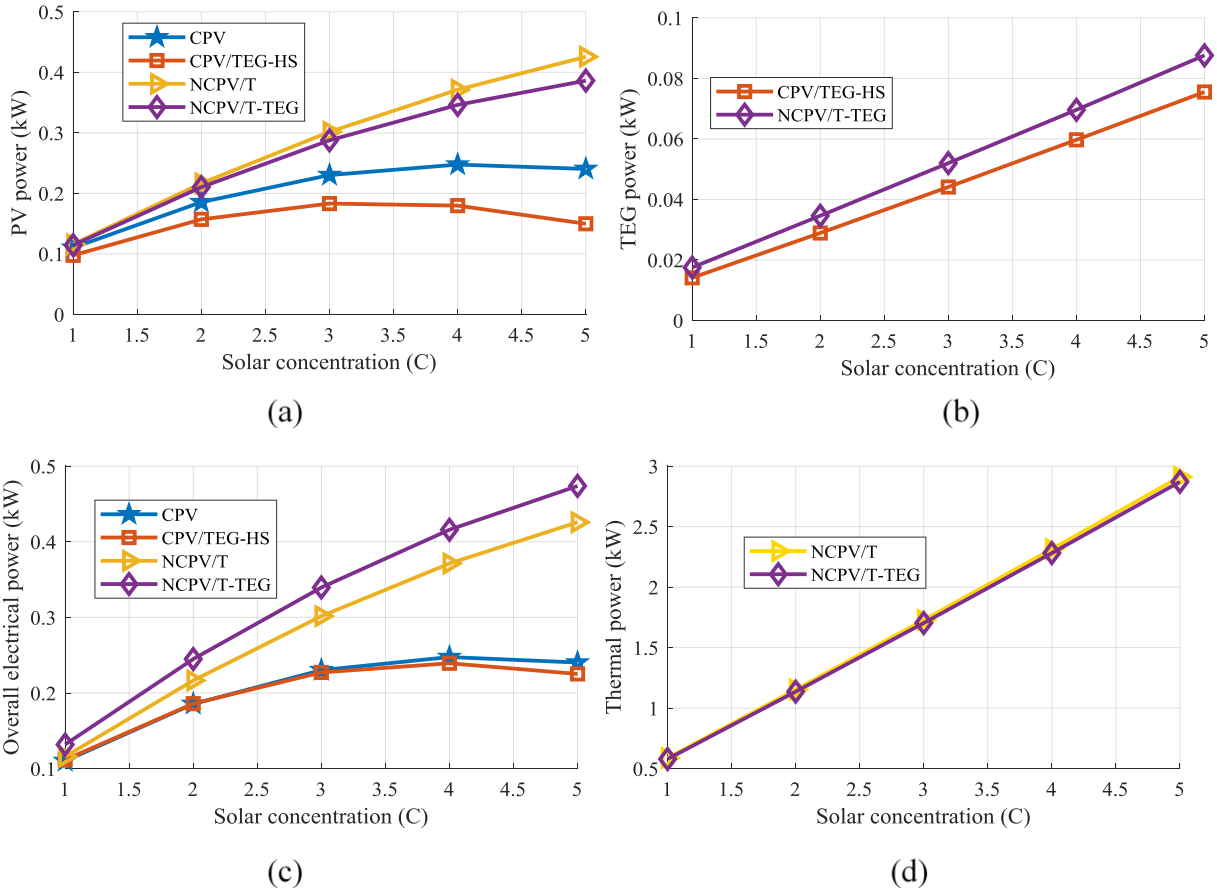
<i>Design</i>	<i>CPV</i>	<i>CPV/TEG-HS</i>		<i>NCPV/T</i>		<i>NCPV/T-TEG</i>		
<i>C</i>	$T_{pv}$	$T_{pv}$	$\Delta T$	$T_{pv}$	$T_f$	$T_{pv}$	$\Delta T$	$T_f$
1	53.39	63.45	1.10	38.16	38.57	40.65	1.35	38.35
2	72.52	90.57	2.25	50.53	51.43	55.42	2.65	50.99
3	91.07	116.05	3.42	62.85	64.45	70.20	3.96	63.79

4	109.00	140.02	4.61	75.13	77.63	85.00	5.30	76.76
5	126.31	162.63	5.82	87.33	90.95	99.76	6.66	89.86

1 As it can be seen from Table 5, the PV module temperature has increased when the solar  
2 concentration ratio is increased. It can be see as well the use of TEG module without effective  
3 cooling system has negative effect on the performance of the PV cells in case of CPV/TEG-HS  
4 system. However, by using nanofluid in NCPV/T-TEG instead of heat sink, the PV cells'  
5 temperature has been reduced by a factor of ~38.5%, and 21% compared to CPV/TEG-HS and  
6 CPV, respectively.

7 The use of solar concentrator technology helps to magnify the incident radiation. The  
8 electrical and thermal performance of the proposed system as well as other three configurations  
9 under concentrated solar approach have been analyzed. It can be seen from Fig. 5 that the overall  
10 system performance, including PV cells, TEG module, and thermal unit, was improved with the  
11 increase in solar concentration ratio. As it can be seen form Fig. 5, at low solar concentration  
12 ratio,  $C < 2$ , all the configurations demonstrated almost similar electrical and thermal  
13 performance. However, at  $C = 5$ , the NCPV/T and NCPV/T-TEG performed better than the  
14 conventional configurations. For instance, the electrical output from PV cells in CPV/TEG-HS  
15 system reached its optimal value at  $C = 3$ , then any increase in  $C$ , the electrical output of the PV  
16 module drops due to the low performance of PV cells at high temperature. This is also due to the  
17 fact that TEG module slows down the heat transfer, as well because of the low cooling efficiency  
18 of the heat sink placed under the TEG module. The approach of using nanofluid as a coolant in  
19 NCPV/T and NCPV/T-TEG prevent the PV cells to be heated up ensuring better electrical  
20 performance compared to CPV-alone and CPV/TEG-HS. In addition, from the Fig. 5(b), the  
21 estimated performance of TEG module in NCPV/T-TEG found to be better than CPV/TEG-HS  
22 due the same reason.

1



2

3 **Figure 5:** Impact of solar concentration variation on (a) PV electrical power output, (b) TEG  
 4 electrical power output, (c) overall electrical power output and (d) thermal power output. The  
 5 depicted data are calculated under the following condition;  $T_{am} = 35^{\circ}C$ ,  $ws = 1.5 m/s$ . In  
 6 addition, for NCPV/T and NCPV/T-TEG the  $\dot{m}=0.0104kg/s$ ,  $\phi = 0.001$ .

7 The thermal performance of the proposed system has been found roughly similar to that in  
 8 NCPV/T system at low solar concentration ratio, and slightly lower at  $C = 4$  onward.

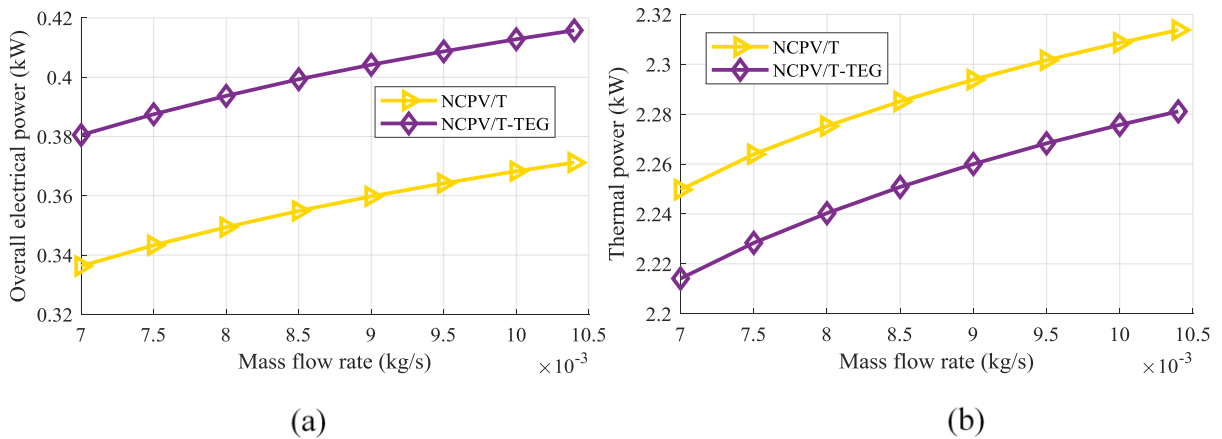
9 Overall, using solar concentration, TEG module, and nanofluid based coolant in the proposed  
 10 system helps to optimize electrical energy for both TEG module and PV cells compared to other  
 11 configurations, as shown in Fig. 5 (c).

### 12 3.4. Impact of Nanofluid parameters

1 After investigating the effect of variation of the ambient conditions, including; temperature, wind  
 2 speed and solar radiation intensity, the next case study is to analyze the effect of nanofluid  
 3 parameters such as mass flow rate and volume fraction, on the electrical and thermal  
 4 performance of the present NCPV/T-TEG against NCPV/T configuration.

### 5 3.4.1. Mass flow rate

6 The mass flow rate is a key parameter for the performance investigation of the proposed  
 7 configuration. Generally, the optimum value of mass flow rate depends on the desired output of  
 8 the system. In this section, thermal and electrical response of the proposed system due to  
 9 variation of mass flow rate has been carried out. It can be seen from Fig.6 (a) that the increase in  
 10 mass flow rate of nanofluid has a positive effect on the electrical power output for both NCPV/T  
 11 and NCPV/T-TEG system. Moreover, thermal output performance has been improved as well  
 12 when mass flow rate is increased. This is due to the enhanced thermal properties of the CNT  
 13 nanofluid.



14 (a) (b)  
 15 **Figure 6:** Impact of Mass flow rate on (a) electrical power (b) thermal power for the physical  
 16 configuration NCPV/T and NCPV/T-TEG, under the following condition:  $ws = 1.5 \text{ m/s}$  ,  
 17  $T_{am} = 35^\circ\text{C}$ ,  $\phi = 0.001$ ,  $C = 4$ .

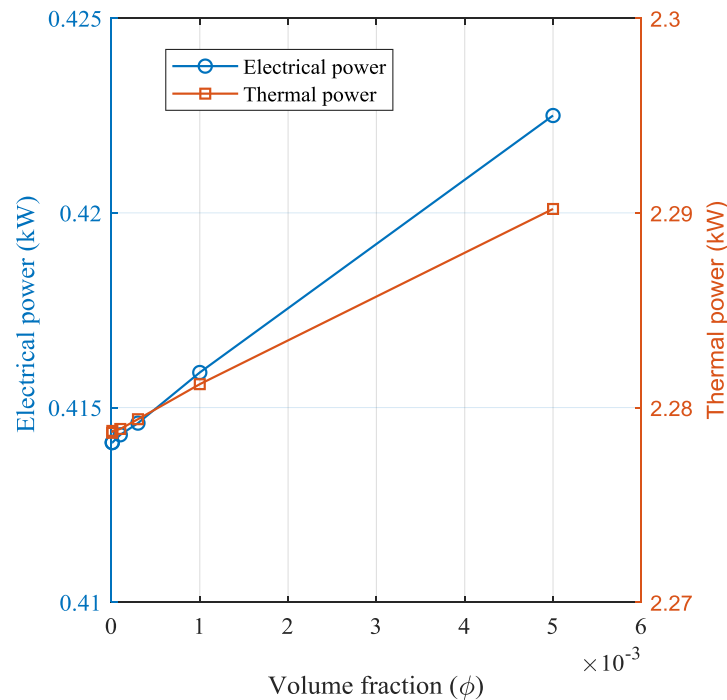
18 Integrating a TEG module into the NCPVT/T-TEG system, overall electrical power output found  
 19 to be improved compared to NCPVT/T system. Despite the thermal outperformance in  
 20 NCPVT/T, the additional electrical gain generated in NCPVT/T-TEG is more valuable than extra

1 thermal energy in NCPVT/T system. This is due to the fact that thermal energy is low grade  
2 energy than electrical energy.

### 3 3.4.2. Volume fraction impact

4 The cooling performance of the nanofluid coolant depend on mass flow rate, nanoparticle  
5 concentration, and thermophysical properties of the base fluid.

6 To investigate the effect of the volume fraction on the overall electrical and thermal  
7 performances of the NCPV/T-TEG hybrid system, a numerical simulation of volume fraction  
8 variation of the thermal nanofluid coolant has been conducted. The obtained output performance  
9 are shown in Fig.7.



10

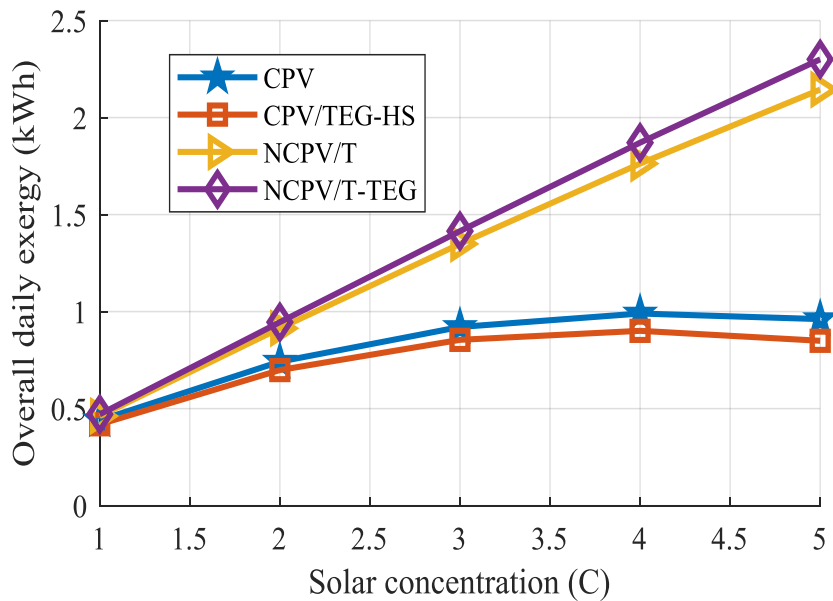
11 **Figure 7:** Impact of volume fraction on (a) electrical power (b) thermal power for the physical  
12 configuration NCPV/T and NCPV/T-TEG, under the condition:  $w_s = 1.5 \text{ m/s}$ ,  $T_{am} = 35^\circ\text{C}$ ,  
13  $\dot{m}=0.0104\text{kg/s}$ ,  $C = 4$ .

14 As it can be seen from Fig.7, increasing the volume fraction of nanoparticle results in a positive  
15 effect on both electrical and thermal performance. This is due to the fact that increasing the  
16 volume fraction of nanoparticles improves the thermal conductivity of the nanofluid, leading to a  
17 batter heat transfer coefficient between the nanofluid and the TEG module. However, the

1 increase in volume fraction beyond an optimal value will results in increase of dynamic  
2 viscosity, consequently the pumping power increase which reduces the overall performance of  
3 the system. Therefore, in this study the value of volume fraction has been limited to 0.1% to  
4 avoid pumping power penalty.

### 5 3.6. Exergy performance

6 The exergy analysis has revealed that the NCPV/T-TEG hybrid system performs batter than  
7 other configurations. It has to be noted that the daily exergy in NCPV/T-TEG and NCPV/T  
8 system is a combination of electrical and thermal exergy. In addition, the daily exergy for the all  
9 configurations has been calculated based on four operating hours under a solar radiation of 992  
10  $W/m^2$ , ambient temperature of  $35^\circ C$ , and wind speed of  $1.5m/s$ . These ambient conditions are  
11 close to those of a tropical region in Southeast Asia.



12

13

**Figure 8:** Daily exergy for the forth configurations.

14 From Fig 8, it can be seen that the daily exergy increases when the solar concentration increases  
15 for all the configurations. The NCPV/T-TEG hybrid system generates the highest amount of  
16 daily exergy against other conventional technologies. In instance, at  $C = 5$  the total exergy  
17 produced in NCPV/T-TEG has been found to be 2302  $Wh$ . This include 1240  $Wh$  form PV  
18 module, 317  $Wh$  form TEG, and 743 $Wh$  from thermal nanofluid. It has to be noted that to keep

1 the nanofluids at liquid state for the configurations NCPV/T and NCPV/T-TEG, the concentration  
2 ratio  $C$  must remain lower than 5.

3 The optimal operating  $C$  in CPV and CPV/TEG-HS system is defined according to maximum  
4 power could be delivered by the PV cells. This is to say, any increase of  $C$  above 4, the output  
5 power will drop due to PV cells temperature. This limitation has been easily avoided in NCPV/T  
6 and further in NCPV/T-TEG systems due to CNT based effective nanofluid cooling system used  
7 in both hybrid systems.

8 The engineering solution by combining TEG and nanofluid in NCPV/T-TEG system has resulted  
9 in better energy performance than other configurations. However, one can note that the amount  
10 of electrical power generated by the TEG module is very low due to the usage of a commercial  
11 TEG module which has very limited performance compared to the lab scale TEG module. The  
12 latter has better efficiency, but not affordable for everyone. With the technological progress, the  
13 future TEG will offer better conversion rate than the current TEG available in the market. Thus,  
14 integrating an advance TEG module in the proposed design of NCPV/T-TEG hybrid system will  
15 result in more daily exergy production.

#### 16 **4. Conclusion**

17 In this study, a novel design of a nanofluid-based CPV/T-TEG hybrid system is proposed to  
18 improve solar energy conversion rate. The TEG helps to maximize the electrical energy of the  
19 proposed configuration and nanofluid-based channel is designed to act as a coolant under the  
20 TEG module and collect useful energy in the form of heat. The analytical analysis of NCPV/T-  
21 TEG system has confirmed the overall performance advantages of combining TEG technology  
22 with PV cells using nanofluid as a cooling strategy.

23 The main conclusions based on the results of the present study are summarized as follows:

24 a) In the CPV/TEG-HS system configuration, a degradation in the overall performance of  
25 the PV cell has been identified. This is due to thermal barrier caused by the TEG module, and  
26 limitation in the cooling power of heat sink. Whereas, the nanofluid-based coolant in the  
27 NCPV/T-TEG system reduced the negative impact of the TEG on the PV cell and achieved a  
28 significant gradient of temperature leading to maximize the overall electrical energy of the  
29 system.



b) It was found that in NCPV/T-TEG configuration the electrical performance is higher by ~10 %, ~47.7 % and ~49.5 % against NCPV/T, CPV and CPV/TEG-HS systems, respectively. However, the overall thermal energy of the NCPV/T-TEG was found lower by ~3% compared with NCPV/T system.

c) The NCPV/T-TEG configuration has been found to be able to produce 2.3 kWh of exergy daily, whereas 0.96, 0.84 and 2.17 kWh of daily exergy was obtained in cases of conventional CPV, CPV/TEG-HS, and NCPV/T, respectively.

d) Based on the results of the present study, it was found that the use of nanofluid-based coolant approach provides a better option to control the energy production (i.e. electrical and thermal energy in the NCPV/T-TEG) by adjusting the nanofluid parameters (i.e. mass flow rate and volume fraction), compared to other cooling process.

To sum up, a novel nanofluid based CPV/T combined with a thermoelectric generator has been developed and analyzed. According to its outstanding performance, it is believed that the present proposed NCPV/T-TEG hybrid system could be one of the best renewable energy technology solution to promote the concept of sustainable development, smart city, and to electrify regions where their connection to grid is economically not feasible.

## Acknowledgment

The authors would like to gratefully acknowledge the funding support provided by Universiti Teknikal Malaysia Melaka under PJP/2016/FKE/HI5/S01482. Abdelhak Lekbir would like to thank Universiti Teknikal Malaysia Melaka for providing PhD scholarship under the UTeM Zamalah Scheme.

## Appendix

All the coefficients and parameters used in the present paper summarized in this appendix:

$$h_{eq(c-am)} = h_{rc-am} + h_{c-am} \quad (A.1)$$

$$h_{rc-am} = \frac{\sigma \varepsilon_c (T_c^4 - T_{sky}^4)}{T_c - T_{am}} \quad (A.2)$$

where  $T_{sky}$  is the sky's temperature evaluated using Daguene's formula [26]

$$T_{sky} = [T_{am}^4 (1 - 0.261 \exp(-7.77 \times 10^{-4} (T_{am} - 232)^2))]^{0.25} \quad (A.3)$$

$$h_{c-am} = \frac{Nu_{c-am}K_{am}}{L_c} \quad (A.4)$$

1 The Nusselt number is calculated using the correlation proposed by Sparrow et al. [27]

$$Nu_{c-am} = 0.86Re_{am}^{1/2}Pr_{am}^{1/3} \quad (A.5)$$

$$hr_{c-pv} = \frac{\sigma\varepsilon_c\varepsilon_v(T_c^2+T_{pv}^2)(T_c+T_{pv})}{\varepsilon_c+\varepsilon_{pv}-\varepsilon_c\varepsilon_{pv}} \quad (A.6)$$

$$h_{p-n} = \frac{Nu_nK_n}{D_h} \quad (A.7)$$

2 The Nusselt number  $Nu_n$  is determined as follow: [25]

$$Nu_n = 7.54 + \frac{0.03Re_nPr_n\frac{D_h}{l}}{1+0.016(Re_nPr_n\frac{D_h}{l})^{2/3}} \quad (A.8)$$

$$Re_n = \frac{\dot{m}_n D_h}{l \varepsilon_n \mu_n} \quad (A.9)$$

3 The average heat transfer coefficient of the heat sink taken from the reference.[12]

$$h_{convf} = \frac{0.037L^{-1/5}\rho CpU_\infty^{4/5}}{\nu^{-1/5}Pr^{2/3}} \quad (A.10)$$

4

## 5 References

- 6 [1] A. McCrone, U. Moslener, F. D’Estais, and C. Grünig, “Global Trends in Renewable  
7 Energy Investment 2017,” *Frankfurt Sch. UNEP Collab. Cent. Clim. Sustain. Energy*  
8 *Financ.*, p. 90, 2017.
- 9 [2] REN21, *Renewables 2017: global status report*, vol. 72, no. October 2016. 2017.
- 10 [3] V. V. Tyagi, N. A. A. Rahim, N. A. Rahim, and J. A. L. Selvaraj, “Progress in solar PV  
11 technology: Research and achievement,” *Renew. Sustain. Energy Rev.*, vol. 20, pp. 443–  
12 461, 2013.
- 13 [4] K. Drew, L. M. Brown, A. Cole, K. Heasman, T. Bruton, and A. Street, “Front dicing  
14 technique for pre-isolation of concentrator silicon solar cells,” *Sol. Energy*, no. September,  
15 pp. 6–10, 2010.
- 16 [5] P. J. Lunde, *Solar thermal engineering: Space heating and hot water systems*. 1980.
- 17 [6] A. Makki, S. Omer, and H. Sabir, “Advancements in hybrid photovoltaic systems for  
18 enhanced solar cells performance,” *Renew. Sustain. Energy Rev.*, vol. 41, pp. 658–684,  
19 2015.
- 20 [7] W. G. J. H. M. van Sark, “Feasibility of photovoltaic - Thermoelectric hybrid modules,”  
21 *Appl. Energy*, vol. 88, no. 8, pp. 2785–2790, 2011.
- 22 [8] J. Lin, T. Liao, and B. Lin, “Performance analysis and load matching of a photovoltaic-  
23 thermoelectric hybrid system,” *Energy Convers. Manag.*, vol. 105, pp. 891–899, 2015.

- 1 [9] D. N. Kossyvakis, G. D. Voutsinas, and E. V. Hristoforou, "Experimental analysis and  
2 performance evaluation of a tandem photovoltaic-thermoelectric hybrid system," *Energy*  
3 *Convers. Manag.*, vol. 117, pp. 490–500, 2016.
- 4 [10] W. Zhu, Y. Deng, Y. Wang, S. Shen, and R. Gulfam, "High-performance photovoltaic-  
5 thermoelectric hybrid power generation system with optimized thermal management,"  
6 *Energy*, vol. 100, no. April, pp. 91–101, 2016.
- 7 [11] G. Li, X. Zhao, and J. Ji, "Conceptual development of a novel photovoltaic-thermoelectric  
8 system and preliminary economic analysis," *Energy Convers. Manag.*, vol. 126, no.  
9 October, pp. 935–943, 2016.
- 10 [12] G. Li *et al.*, "Performance analysis on a solar concentrating thermoelectric generator using  
11 the micro-channel heat pipe array," *Energy Convers. Manag.*, vol. 112, pp. 191–198,  
12 2016.
- 13 [13] M. Mohsenzadeh, M. B. Shafii, and H. Jafari mosleh, "A novel concentrating  
14 photovoltaic/thermal solar system combined with thermoelectric module in an integrated  
15 design," *Renew. Energy*, vol. 113, pp. 822–834, 2017.
- 16 [14] S. Soltani, A. Kasaeian, T. Sokhansefat, and M. B. Shafii, "Performance investigation of a  
17 hybrid photovoltaic/thermoelectric system integrated with parabolic trough collector,"  
18 *Energy Convers. Manag.*, vol. 159, no. December 2017, pp. 371–380, 2018.
- 19 [15] C. B. Vining, "An inconvenient truth about thermoelectrics TL - 8," *Nat. Mater.*, vol. 8  
20 VN-re, no. 2, pp. 83–85, 2009.
- 21 [16] S. Nag, A. Dhar, and A. Gupta, *Exhaust Heat Recovery Using Thermoelectric*  
22 *Generators : A Review*. 2018.
- 23 [17] A. N. Al-Shamani, K. Sopian, S. Mat, H. A. Hasan, A. M. Abed, and M. H. Ruslan,  
24 "Experimental studies of rectangular tube absorber photovoltaic thermal collector with  
25 various types of nanofluids under the tropical climate conditions," *Energy Convers.*  
26 *Manag.*, vol. 124, pp. 528–542, 2016.
- 27 [18] O. Rejeb, M. Sardarabadi, C. Ménézo, and M. Passandideh-fard, "Numerical and model  
28 validation of uncovered nanofluid sheet and tube type photovoltaic thermal solar system,"  
29 *ENERGY Convers. Manag.*, vol. 110, pp. 367–377, 2016.
- 30 [19] S. Hassani, R. A. Taylor, S. Mekhilef, and R. Saidur, "A cascade nanofluid-based PV/T  
31 system with optimized optical and thermal properties," *Energy*, vol. 112, no. August, pp.  
32 963–975, 2016.
- 33 [20] S. Hassani, R. Saidur, S. Mekhilef, and R. A. Taylor, "Environmental and exergy benefit  
34 of nanofluid-based hybrid PV/T systems," *Energy Convers. Manag.*, vol. 123, no.  
35 September, pp. 431–444, 2016.
- 36 [21] D. Jing, Y. Hu, M. Liu, J. Wei, and L. Guo, "ScienceDirect Preparation of highly  
37 dispersed nanofluid and CFD study of its utilization in a concentrating PV / T system,"  
38 *Sol. ENERGY*, vol. 112, pp. 30–40, 2015.
- 39 [22] S. Hassani, R. Saidur, S. Mekhilef, and A. Hepbasli, "A new correlation for predicting the

1 thermal conductivity of nanofluids; using dimensional analysis,” *Int. J. Heat Mass Transf.*,  
2 vol. 90, no. November, pp. 121–130, 2015.

3 [23] W. Duangthongsuk and S. Wongwises, “Comparison of the effects of measured and  
4 computed thermophysical properties of nanofluids on heat transfer performance,” *Exp.*  
5 *Therm. Fluid Sci.*, vol. 34, no. 5, pp. 616–624, 2010.

6 [24] T. T. Chow, G. Pei, K. F. Fong, Z. Lin, A. L. S. Chan, and J. Ji, “Energy and exergy  
7 analysis of photovoltaic-thermal collector with and without glass cover,” *Appl. Energy*,  
8 vol. 86, no. 3, pp. 310–316, 2009.

9 [25] G. A. Cengel YA, *heat and mass transfer: fundamentals & applications*, 4th ed,McG.  
10 2011.

11 [26] Michel Daguene, *Les Séchoirs solaires: théorie et pratique*. UNESCO, 1985.

12 [27] J. W. R. and E. A. M. E. M. Sparrow, “Effect of Finite Width on Heat Transfer and Fluid  
13 Flow about an Inclined Rectangular Plate,” *J. Heat Transf.*, vol. 101, no. 2, pp. 199–204,  
14 1979.

15  
16  
17  
18  
19  
20  
21